Photoinduced Electron Transfer (PET) Based Zn2+ Fluorescent Probe: Transformation of Turn-On Sensors into Ratiometric Ones with Dual Emission in Acetonitrile

ARTICLE *in* THE JOURNAL OF PHYSICAL CHEMISTRY A · NOVEMBER 2011

Impact Factor: 2.69 · DOI: 10.1021/jp209061f · Source: PubMed

3 AUTHORS, INCLUDING:

Pichandi Ashokkumar
University of Strasbourg
13 PUBLICATIONS **159** CITATIONS
SEE PROFILE

Perumal Ramamurthy
University of Madras
110 PUBLICATIONS **1,849** CITATIONS
SEE PROFILE

THE JOURNAL OF PHYSICAL CHEMISTRY A

ARTICLE

pubs.acs.org/JPCA

Photoinduced Electron Transfer (PET) Based Zn^{2+} Fluorescent Probe: Transformation of Turn-On Sensors into Ratiometric Ones with Dual Emission in Acetonitrile

P. Ashokkumar, V. T. Ramakrishnan, and P. Ramamurthy*

National Centre for Ultrafast Processes, University of Madras, Taramani Campus, Chennai-600 113, India

Supporting Information

ABSTRACT: Ratiometric sensors for the detection of metal ions have gained increasing attention due to its self-calibration tendency for the environmental effects. In this context, we have synthesized and characterized a dual emitting ratiometric Zn^{2+} probe (**1**) having acridinedione as a fluorophore and *N*,*N*-bis(2-pyridylmethyl)amine (BPA) as a receptor unit. Existence of two different conformation of the molecule with photoinduced electron transfer (PET) from amine moiety to the acridinedione fluorophore leads to dual emission, namely locally excited (425 nm) and anomalous charge transfer emission (560 nm) in aprotic solvents. In the presence of one equivalent of Zn^{2+}, a 15-fold fluorescence enhancement in the locally excited state together with the quenching of charge transfer emission is observed. The intensity changes at the two emission peaks allow a ratiometric detection of Zn^{2+} under PET signaling mechanism. The utilization of PET process for the ratiometric fluorescence change will further signify the importance of PET mechanism in sensing action. Addition of Zn^{2+} to **1** in acetonitrile/water mixtures shows a single emission peak with fluorescence enhancement.

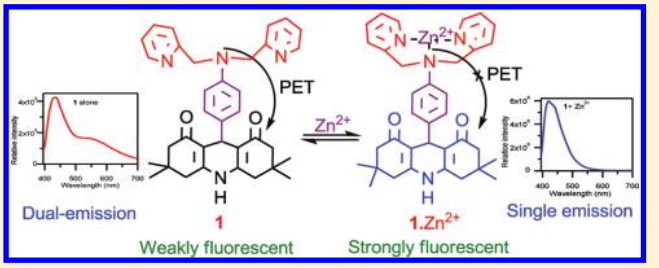

I. INTRODUCTION

Among the trace elements involved in human metabolism, Zn^{2+} is the most ubiquitous, and its physiological importance has long been recognized.[1] Generally, the total concentration of Zn^{2+} in different types of cells is quite varied, ranging from the nM level to ~0.3 mM.[2] Thus, the highly selective, sensitive and reversible detection of Zn^{2+} ions is of vital importance. In this context, the development of fluorescence based sensors attracted more attention due to its advantages such as high sensitivity of the detection down to single molecule, local observation by fluorescence imaging with subnanometer spatial resolution and remote sensing by using optical fibers with a molecular sensor immobilized at the tip.[3] Until now, a variety of fluorescent Zn^{2+} sensors[4−9] have been documented, based on photoinduced electron transfer (PET),[5] internal charge transfer (ICT),[6] excimer/exciplex formation,[7] chelation-enhanced fluorescence (CHEF),[8] and fluorescence resonance energy transfer (FRET)[9] mechanisms. To date, most of the available Zn^{2+} fluorescent sensors rely on the PET mechanism, which exhibits an increase in the emission intensity, but show little or no spectral shift in both absorption and emission spectra.[10] Lippard and co-workers reported an elegant example of fluorescein-based Zn^{2+} chemosensors (Zinpyr-1) containing the Zn^{2+} binding moiety, bis(2-pyridylmethyl)amine (BPA).[11] BPA is used as a chelator for Zn^{2+} due to its highly specific binding over other metal ions, and a favorable kinetic and thermodynamic properties, which result in quick formation of a stable Zn^{2+} complex.[12] Furthermore, they can be readily incorporated into a fluorophore, which simplifies the synthetic route. BPA can effectively quench the emission of the fluorophore via PET; upon addition of Zn^{2+} ions, fluorescence enhancement is observed owing to the formation of BPA-Zn^{2+} complex, which can efficiently block the PET process. Because of the unchanged absorption and emission maxima, ratiometric detection under PET signaling mechanism is not achieved so far. Only a very few PET based sensors show emission spectral shift due to the repulsive electrostatic interaction between the excited-state dipole of the sensor molecule and metal ion.[13] Ratiometric detection by utilizing both PET and ICT mechanisms is achieved.[14] Similarly, a ratiometric fluorescence output by exploiting PET and FRET is also obtained;[9a] however, a ratiometric change solely due to the operation of PET process is not yet reported.

Unfortunately, most of the fluorescent probes reported for Zn^{2+} are based on single emission intensity changes, which tend to be affected by a variety of factors, such as instrumental efficiency, probe molecule concentration, its stability under photoillumination, and microenvironment around probe molecule. These limitations can be circumvented by the use of ratiometric probes, which are less prone for such problems. Ratiometric fluorescent probes involve changes in the ratio of the two emission peaks upon the addition of an analyte, which are beneficial for increasing the dynamic range and providing built-in

Received: September 20, 2011
Revised: November 4, 2011
Published: November 09, 2011

Scheme 1. Structure of ADD Dyes

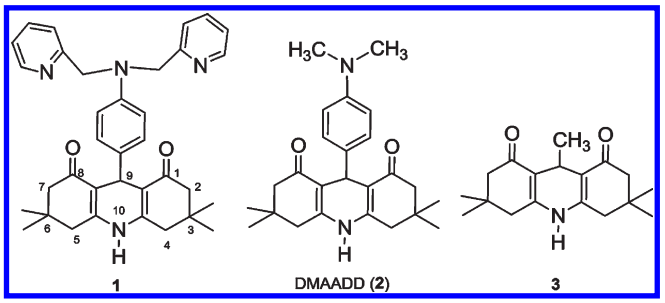

correction for environmental effects.[15] Ratiometric probes for metal ions have been the subject of a series of investigations in recent years.[16] So far, the reported ratiometric sensors utilized ICT process, which exhibits a shift in both the absorption and emission maxima.[6a] For example, cation complexation with an electron donor group reduces the electron-donating character and thus reducing the conjugation, which results in a blue shift of the absorption and emission maxima together with a decrease of the molar absorptivity. In contrast, the metal ion binding to the acceptor group enhances its electron-withdrawing character, which results in a red shift in both absorption and emission maxima. However, most currently available ratiometric sensors for Zn^{2+} are still not satisfactory due to the small emission shifts.[17] Here, we report our new strategy for the development of the ratiometric fluorescent sensor based on the PET signaling mechanism by using acridinedione (ADD) as a fluorophore and BPA moiety as a Zn^{2+} chelator. These two moieties are linked covalently through nonconjugated fashion, which minimizes the electronic communication between the receptor unit and fluorophore moiety in the ground state. On excitation, an efficient PET occurs from BPA to ADD fluorophore, which results in a lower fluorescence quantum yield with dual emission, one peak at 425 nm and another peak at 560 nm in aprotic solvents. The large difference in the peak position will be an advantage for the ratiometric detection of Zn^{2+}.

Recently, ADD, a class of laser dye has been exploited as a signaling unit in sensor molecule due to the occurrence of both PET and ICT in a single molecule.[18] Here, we have synthesized BPA linked ADD (**1**), which exhibits a dual emission in aprotic solvents due to the locally excited (LE) and PET promoted charge transfer (CT) state. The origin of the dual emission has been confirmed by comparing with two other ADD derivatives, which have *p*-dimethylaminobenzene and methyl groups at the ninth position of the ADD moiety (Scheme 1). In the presence of Zn^{2+}, compound **1** shows a fluorescence enhancement in the LE state with the disappearance of PET promoted CT state that allows a selective ratiometric detection of Zn^{2+} by utilizing PET signaling mechanism.

II. EXPERIMENTAL SECTION

General Information. Dimedone was purchased from Lancaster (India) Ltd. 4-Nitrobenzaldehyde and 2-(chloromethyl)pyridine hydrochloride and all metal ions as their perchlorates were purchased from Sigma Aldrich Chemicals Pvt. Ltd. The solvents used for the spectral studies were of HPLC grade. Absorption spectra were recorded using Agilent 8453 diode array spectrophotometer. Emission; excitation and 3D contour spectra were recorded on HORIBA JOBIN YVON Fluoromax-4P spectrometer. Fluorescence quantum yield was determined by exciting the sample at 366 nm with the use of quinine sulfate as the standard (ϕ_f = 0.546 in 0.1 N H_2SO_4). Fluorescence decays were recorded by using an IBH time-correlated single-photon counting spectrometer as reported elsewhere.[19] NMR spectra were recorded on JEOL 500 MHz instrument in deuterated solvents as indicated; chemical shifts are reported in ppm and coupling constants ($J_{X\text{-}X'}$) are reported in Hz. ESI-MS were performed on an ECA LCQ Thermo system with ion-trap detection in positive and negative mode. Elemental analyses (C, H, and N) were taken on a Euro EA Elemental analyzer.

General Procedure for Metal Ion Binding Studies. Compound **1** was dissolved in the respective solvents. Metal perchlorate stock solutions (9.11×10^{-3} M) were prepared in acetonitrile and the titrations were carried out by adding small volumes (1−5 μL) of the metal ion to dye (3.5 mL) in quartz cuvette. After the addition of metal ion to the cuvette, using a microliter syringe, the solution was shaken well and kept for 1 min before recording any measurements. Complex stoichiometry has been determined from the continuous variation technique (Job's plot),[20] based on the difference in integral area of fluorescence spectra ΔF ($\Delta F = F_0 - F$) of dye observed in the presence of metal ions. Equimolar solutions of **1** and metal ions were prepared and mixed to standard volumes and proportions in order that the total concentration remained constant. ΔF values were calculated by measuring the integral area of fluorescence spectra of dye in the absence (F_0) and presence (F) of the corresponding concentration of metal ion. Subsequently, ΔF were plotted for the metal ion against mole fraction (xi = [dye]/([dye] + [metal ion])).

Synthesis. The synthetic routes to sensor **1** is outlined in Scheme 2. Compounds **1a**−**c** and the other compounds (**2** and **3**) employed in this investigation as illustrated in Scheme 1 were synthesized following the procedure reported in the literature.[18a,21]

*9-(4-(Bis(pyridine-2-ylmethyl)amino)phenyl)-3,3,6,6-tetramethyl-3,4,6,7,9,10-hexahydro-1,8(2H,5H)acridinedione (**1**).* A mixture of amino-acridinedione **1c** (0.75 g, 2.0 mmol), 2-(chloromethyl)pyridine hydrochloride (0.67 g, 4.1 mmol), and sodium carbonate (0.47 g, 7.4 mmol) in 20 mL ethanol was refluxed under a nitrogen atmosphere for 12 h. The reaction mixture was concentrated by evaporating the solvent; the residue was dissolved in 20 mL of aqueous solution of sodium hydroxide and extracted three times with dichloromethane. The combined organic layer was dried with magnesium sulfate, filtered and evaporated in vacuo. The crude product was purified by silica gel chromatography using $CHCl_3$/MeOH (97:3) as an eluent to isolate pure compound **1** (0.62 g, 57%) as a yellow powder. Mp 209−211 °C; IR (KBr): 3273 [br. (NH)], 1636 [vs conj. CO)], 1367 [s. (conj. −C═C−)] cm^{-1}; ^{1}H NMR (500 MHz, DMSO-d_6) δ (ppm): 0.81 and 0.94 (2s, 12H, *gem*-dimethyl); 1.94 and 2.08 (2d, 4H, J = 16.1 Hz, C_2 and C_7 $-CH_2$); 2.26 and 2.33 (2d, 4H, J = 17.0 Hz, C_4 and C_5 $-CH_2$); 4.61 (s, 1H, C_9−H); 4.69 (s, 4H, $-CH_2$); 6.39 (d, 2H, J = 8.5 Hz, ADD Ar−H); 6.80 (d, 2H, J = 8.6 Hz, ADD Ar−H); 7.20 (m, 4H, Ar−H); 7.65 (t, 2H, Ar−H); 8.49 (d, 2H, J = 4.5 Hz, Ar−H); 9.12 (s, 1H, NH); ^{13}C NMR (125 MHz, DMSO-d_6) δ (ppm): 27.6 (CH_3), 29.4 (CH_3), 30.9 (CH), 32.7 (C), 40.5 (CH_2), 50.8 (CH_2), 57.4 (CH_2), 111.9 (CH), 112.3 (C), 121.6 (CH), 122.6 (CH), 128.6 (CH), 136.0 (C), 137.2 (CH), 146.4 (C), 149.4 (C), 149.8 (CH), 159.8 (CH), 195.0 (C); MS (ESI): m/z = 547.81 $[M + 1]^+$; elemental analysis (%) calcd for $C_{35}H_{38}N_4O_2$ (546.70): C 76.89, H 7.01, N 10.25. Found: C 76.78, H 7.04, N 10.29.

Scheme 2. Synthetic Routes to Compound 1

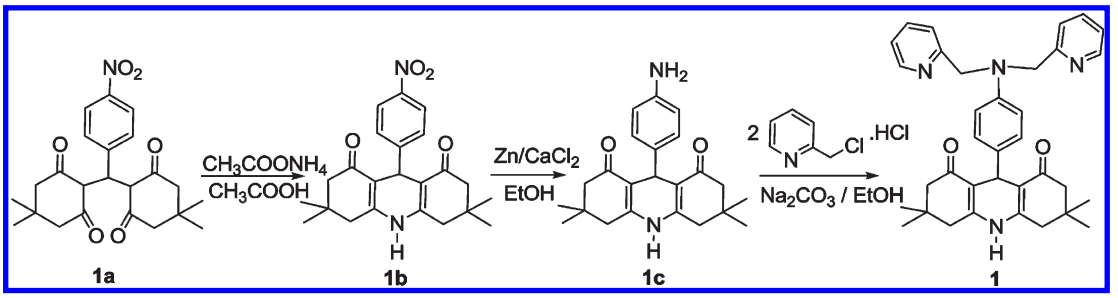

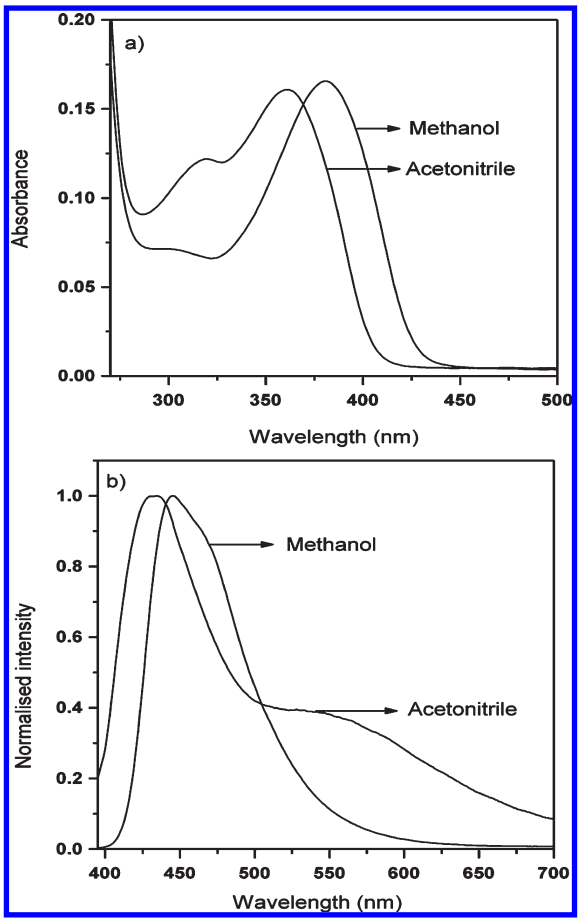

Figure 1. (a) Absorption and (b) emission spectra of **1** in methanol and acetonitrile.

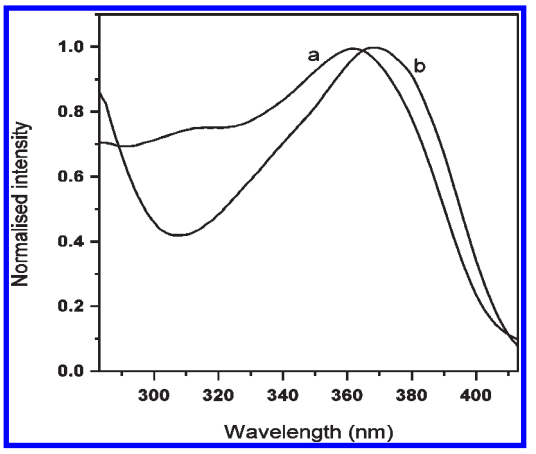

Figure 2. Fluorescence excitation spectra of **1** in acetonitrile: (a) λ_{em} at 560 nm, (b) λ_{em} at 425 nm.

III. RESULTS AND DISCUSSION

(a). Photophysical Studies. Absorption and emission spectral studies of **1** have been carried out in a series of protic and aprotic solvents, which show two sets of results. The representative spectra are presented in Figure 1. In aprotic solvents, **1** exhibits a strong absorption around 360 nm due to the ICT from the ring nitrogen to ring carbonyl oxygen center within the ADD fluorophore. A shoulder around 315 nm is also observed, which is assigned to the electronic transition of BPA group. However in protic solvents, the shoulder appeared in the blue-shifted region due to the protonation of amine moiety. The corresponding emission spectrum was recorded by exciting at its longest wavelength absorption maximum. Compound **1** shows a single emission in protic solvents, whereas in aprotic solvents, it exhibits a dual emission. For example, in acetonitrile a shorter wavelength LE fluorescence at 425 nm and a new anomalous longer wavelength CT fluorescence around 560 nm is observed. However, in methanol, a single emission peak is observed at 440 nm. The observed dual emission of **1** in aprotic solvents is similar to the earlier reported DMAADD (**2**) molecule, which has a *p*-dimethylamino group as the electron donor moiety.[22] The existence of two different conformations of DMAADD in the excited state leads to the dual emission in aprotic solvents.

To confirm whether the similar reason is responsible for the dual fluorescence in **1**, we have carried out excitation (Figure 2) and 3D contour spectral studies (Figure S1). The fluorescence excitation spectrum of **1** show two different excitation maximum at 370 and 362 nm, when monitored at emission maximum 425 and 560 nm, respectively. The excitation spectrum recorded at the longer wavelength emission maximum shows a shoulder around 315 nm, whereas such shoulder is not observed in the excitation spectrum recorded at the shorter wavelength emission maximum. So, the emission at 425 nm arises within the ADD fluorophore (LE state); whereas the emission at 560 nm involves BPA group as a donor and ADD moiety as an acceptor. Presence of two different emission species was further confirmed from 3D contour spectral studies. Compound **1** shows two contours at excitation, emission wavelength 370, 427 and 362, 560 nm that corresponds to LE and CT state, respectively. This clearly confirms the presence of two different emission states of the molecule with different origin of excitation. The existence of two

dx.doi.org/10.1021/jp209061f |*J. Phys. Chem. A* 2011, 115, 14292–14299

different conformation of the same molecule in the excited state leads to the formation of a dual emission in aprotic solvents, namely LE and PET promoted CT state as shown in Scheme 3. In one of the conformations, an efficient PET from the electron-rich amino moiety to the relatively electron-deficient excited state of ADD fluorophore occurs that leads to the formation of a new PET promoted CT state as observed in DMAADD **2**.[22] The observed lower fluorescence quantum yield and shorter fluorescence lifetime (Table 1) of **1** also corroborate the operation of PET process. In acetonitrile, compound **1** shows a fluorescence quantum yield of 0.087 (±5%), which is very low when compared to **3** (0.83 ± 2%), which has a methyl group at the ninth position of the ADD.

Fluorescence decay of **3** obeys single exponential fit with the lifetime of 5.65 ns, whereas **1** shows a biexponential decay (0.51 and 3.28 ns) at all emission wavelengths (Figure S2). The shorter lifetime component is due to the PET promoted CT state and the longer lifetime component is due to the PET quenched LE state. In a similar manner, **2** also shows a biexponential decay (0.66 and 1.98 ns) at emission wavelengths below 530 nm due to the spectral overlap of both the LE and CT states, whereas above 530 nm, only the CT state lifetime of 0.66 ns is observed. This clearly proves that the PET is more efficient in compound **2** compared to **1** that exhibits a strong CT state fluorescence above 530 nm. The observed lower CT/LE state emission intensity ratio of **1** (0.52) compared to **2** (3.85; when both excited at 366 nm) also supports our argument. The presence of strong electron donor group in **2** leads to the effective PET process, but the lack of selective metal ion receptor group limits its usage as a sensor molecule. On the other hand, the presence of selective Zn^{2+} chelator, BPA enables compound **1** as a good candidate for the ratiometric fluorescence sensor.

(b). Metal Ion Binding Studies. Addition of Zn^{2+} to the acetonitrile solution of **1** shows the disappearance of BPA moiety absorption around 315 nm (Figure 3), which indicates that there is an interaction between Zn^{2+} and the receptor unit in the ground state. On the other hand, no change in the ADD absorption maximum is observed, which confirms the absence of any interaction between receptor unit and ADD fluorophore in the ground state. Figure 4 presents the emission spectra of **1** with the addition of Zn^{2+} in acetonitrile. Addition of Zn^{2+} leads

Scheme 3. Dual Fluorescence of Dye 1 and the Zn^{2+} Induced Disappearance of CT Emission

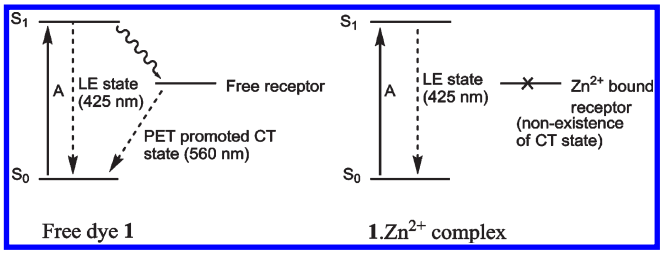

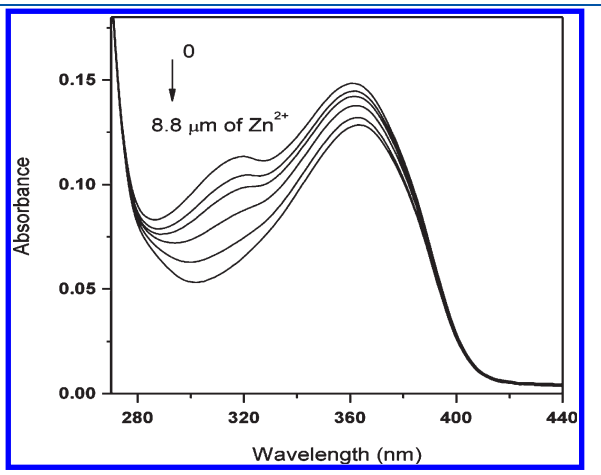

Figure 3. Absorption spectra of **1** (12 μM) upon addition of Zn^{2+} in acetonitrile.

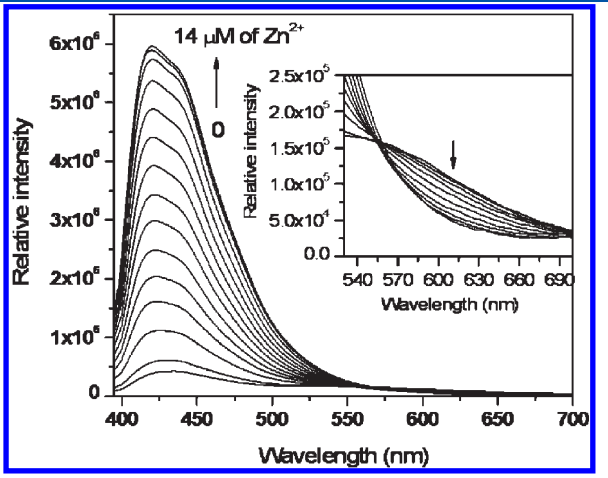

Figure 4. Emission spectra of **1** (12 μM) upon addition of Zn^{2+} in acetonitrile; λ_{ex} = 388 nm. Inset shows the emission spectra in the region of 530−700 nm.

Table 1. Absorption, Emission Maxima, Molar Absorption Coefficient, Fluorescence Quantum Yield, and Fluorescence Lifetime of 1, 2, and 3 in CH_3CN

					τ_f (ns)[b]	
compound	λ_{abs} (nm)	molar extinction coeff. (log ε) M^{-1} cm^{-1}	λ_{em} (nm)	Φ_f[a]	λ_{em} at 425 nm	λ_{em} at 560 nm
1	361	3.85	425, 560	0.087 (±5%)	0.51 (28.7)	0.51 (87.4)
					3.28 (71.3)	3.28 (12.6)
2	362	3.84	424, 550	0.006 (±5%)	0.66 (36.4)	0.66 (100)
					1.98 (63.6)	
3[27]	365	3.94	426	0.83 (±2%)	5.65 (100)	5.65 (100)

[a] Fluorescence quantum yields were determined by exciting the sample at 366 nm using quinine sulfate as the standard (Φ_f = 0.546 in 0.1 N H_2SO_4). [b] λ_{ex} = 370 nm; error in shorter lifetime is ±0.02 ns and in longer lifetime is ±0.03 ns; relative amplitude corresponding to the lifetime is given in the bracket.

dx.doi.org/10.1021/jp209061f |J. Phys. Chem. A 2011, 115, 14292–14299

to a 15-fold enhancement in the LE state fluorescence intensity with the disappearance of CT state fluorescence. Fluorescence intensity saturates when the concentration of Zn^{2+} reaches one equivalent, which shows the 1:1 complexation between receptor and Zn^{2+}, and the stoichiometry was further confirmed from the Job's plot.[20] The Job's plot (Figure 5) showed the maximum changes when the mole fraction of **1** was around 0.5, which is characteristic of a 1:1 stoichiometric host−guest binding. Binding of Zn^{2+} at the BPA moiety alters the conformation of the molecule in to a single one, where PET process does not exist, which results in the disappearance of CT state emission together with the enhancement in the LE state intensity. The emission

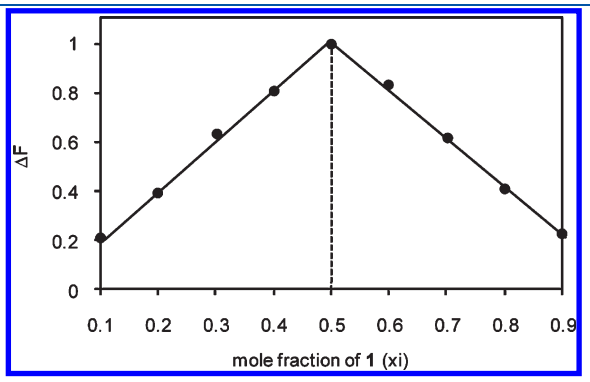

Figure 5. Job's plot for the binding of **1** with Zn^{2+} in acetonitrile; λ_{ex} = 388 nm.

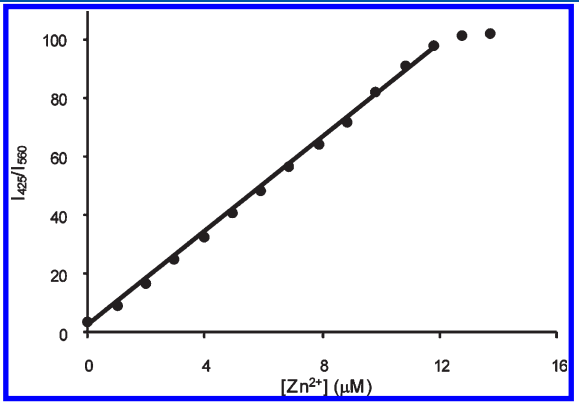

Figure 6. Fluorescence intensity ratio of **1** (12 μM) upon addition of Zn^{2+} in acetonitrile; λ_{ex} = 388 nm.

intensity ratio, I_{425}/I_{560}, increases from 3.3 to 103, when the concentration of Zn^{2+} is varied from 0 to 14 μM (Figure 6). A linear increase in the ratio is observed in the concentration range of 1.0 to 11.8 μM, which enables the quantitative detection under ratiometric response. The large difference (135 nm) in the peak position and the higher enhancement in the fluorescence intensity will be an advantage for ratiometric detection. But, the enhancement of the intensity at 425 nm is more compared to the decrease in the intensity at 560 nm peak, which makes the ratiometric detection is difficult, when compared to other reported derivatives. However, the utilization of PET promoted CT state quenching will be an additional example for the ratiometric detection and it also signifies the usage of PET signaling mechanism for the ratiometric detection. The detection limit (DL) can be calculated with the equation,[23] DL = $3S_0/m$, where "m" is the calibration sensitivity of the fluorescence intensity change ($\Delta F = F_0 - F$) versus [Zn^{2+}], and "S_0" is the standard deviation of the blank signal (F_0) obtained without Zn^{2+}. From this, the lower detection limit was found to be 98 nM in acetonitrile.

Changes in the fluorescence intensity of **1** caused by other metal ions, including Na^+, K^+, Mg^{2+}, Ca^{2+}, Mn^{2+}, Fe^{2+}, Co^{2+}, Ni^{2+}, Cu^{2+}, and Cd^{2+} were also measured as shown in Figure 7a. Addition of paramagnetic transition metal ions such as Co^{2+} and Cu^{2+} shows fluorescence quenching to a different extent (Figures S3 and S4) at both the states and at all concentrations, whereas the addition of Ni^{2+}, Fe^{2+}, Mn^{2+}, and Cd^{2+} shows a relatively lower fluorescence enhancement in the LE state at the lower concentration and fluorescence quenching at the higher concentration, as shown in Figure S5. On the other hand, the CT state fluorescence is quenched at all concentrations. Binding of metal ion at the receptor site suppresses the PET process and results in the LE state fluorescence enhancement, whereas, the direct interaction of transition metal ion with the fluorophore leads to fluorescence quenching.[24] From the above results, it is clear that Cu^{2+} and Co^{2+} did not involve in the binding at the receptor moiety, whereas Ni^{2+}, Fe^{2+}, Mn^{2+}, and Cd^{2+} shows a weak binding at lower concentration. On the other hand, the important biorelated metal ions such as Na^+, K^+, Mg^{2+}, and Ca^{2+}, which often exist at high concentrations in most of the living cells, resulted in a negligible fluorescence change, as compared with that of Zn^{2+} ions. This can be ascribed to the poor coordination capability of these abundant metal ions with BPA receptor. These results also agree quite well with those reported for Zn^{2+} probes based on other fluorophores.[6b,17e] In addition, fluorescence

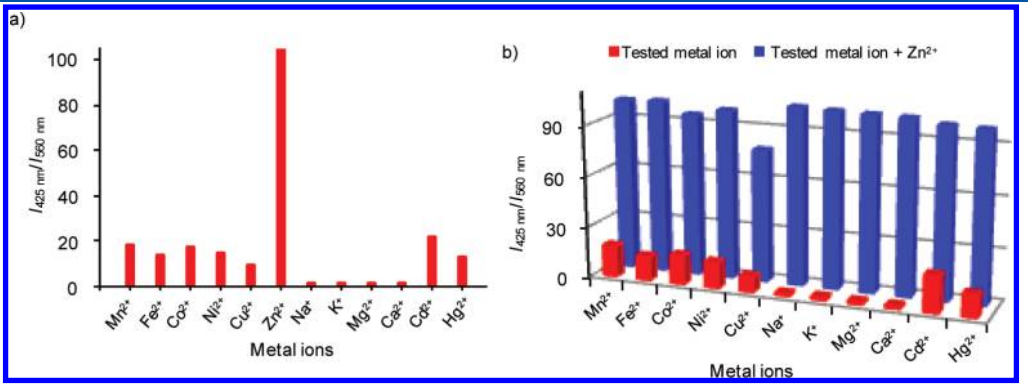

Figure 7. (a) Fluorescence intensity ratiometric response of **1** (12 μM) upon addition of various metal ions (3 equiv to that of Zn^{2+}); (b) Fluorescence intensity ratiometric response of **1** (12 μM) upon addition of Zn^{2+} in the presence of interfered metal ions in acetonitrile; λ_{ex} = 388 nm.

Table 2. Stability Constant of 1 with Various Metal Ions[a] in Acetonitrile and Acetonitrile/Water (80:20, v/v) Mixture

solvent	Mn^{2+}	Fe^{2+}	Ni^{2+}	Zn^{2+}	Cd^{2+}	Hg^{2+}
acetonitrile	3.41×10^3	2.67×10^3	3.25×10^3	2.34×10^5	3.67×10^3	2.57×10^3
acetonitrile/water (80:20, v/v)	1.16×10^3	1.03×10^3	1.30×10^3	5.67×10^4	1.40×10^3	9.83×10^2

[a] Cu^{2+} and Co^{2+} do not involve binding with BPA moiety; Na^+, K^+, Mg^{2+}, and Ca^{2+} show no appreciable change in the fluorescence intensity to measure the stability constant.

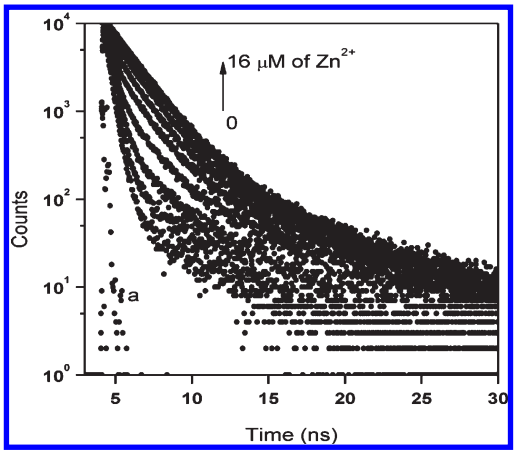

Figure 8. Fluorescence lifetime decay of **1** (12 μM) upon addition of Zn^{2+} in acetonitrile: λ_{ex} = 388 nm, λ_{em} at 560 nm; (a) laser profile.

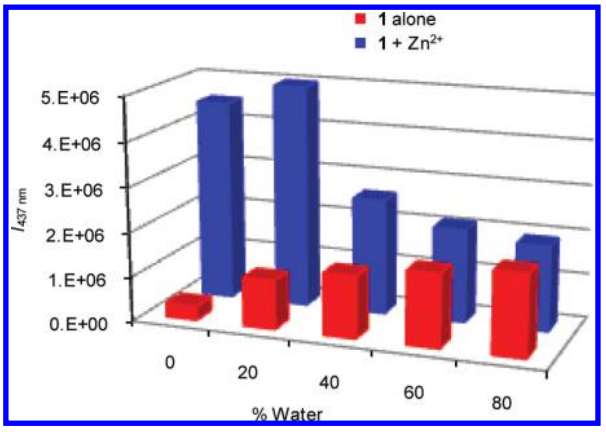

Figure 9. Fluorescence intensity changes (at 437 nm) of **1** (12 μM) as a function of water content in aqueous acetonitrile solution in the absence and presence of Zn^{2+} (18 μM): λ_{ex} = 388 nm.

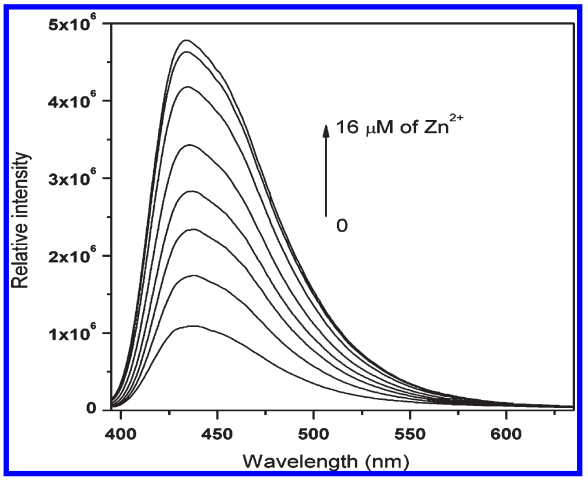

Figure 10. Emission spectra of **1** (12 mM) upon addition of Zn^{2+} in water/acetonitrile (80:20, v/v): λ_{ex} = 388 nm.

spectra of **1** recorded in the presence of Zn^{2+} ions (1.0 equiv) and 3.0 equiv of all the above competing metal ions further revealed that other metal ions, except for Cu^{2+} and Co^{2+} ions, do not interfere with Zn^{2+}-induced fluorescence enhancement. The observed quenching of the fluorescence by Co^{2+} and Cu^{2+} assures that no "false positive" turn-on response would be induced by such metal ions in the analysis of samples. Fluorescence intensity ratio (Figure 7b) of **1** with Zn^{2+} in the presence of above metal ions (except Cu^{2+} and Co^{2+}) is observed to be similar to that of **1** with Zn^{2+} alone (i.e., $I_{425}/I_{560} \sim 100$). The well-known fluorescence quencher, Cu^{2+} ion can directly interact with the ADD fluorophore, thus it can seriously interfere with the fluorescence enhancement of **1** by Zn^{2+} ions. The stability constant of the metal ion complex of **1** is evaluated from the Benesi–Hildebrand plot[25] (Figure S6) of $1/I_0 - I$ against [metal ion]. Among the metal ions investigated, Zn^{2+} shows the binding constant of 2.5×10^5 M^{-1} in acetonitrile, whereas other transition metal ions, except Cu^{2+} and Co^{2+} show a weak binding constant in the range of $2.3 - 3.7 \times 10^3$ M^{-1} as presented in Table 2.

Time-resolved fluorescence studies will provide invaluable information about the system when more than one emitting species contribute to steady-state fluorescence intensities. Such fluorescence lifetime based sensors for Zn^{2+} detection is already reported.[26] Here, we have carried out fluorescence lifetime studies to confirm the involvement of PET process in the fluorescence signaling action. Compound **1** shows 0.51 (87.4%) and 3.28 ns (12.6%), when monitored at emission wavelength of 560 nm. Figure 8 shows the fluorescence decay of **1** with the addition of various concentration of Zn^{2+} in acetonitrile. Addition of Zn^{2+} results in the disappearance of the shorter lifetime component with the formation of a new lifetime component (1.75 ns) along with an increase in the amplitude. Disappearance of the shorter lifetime component confirms the suppression of PET process and hence the disappearance of CT state emission in the Zn^{2+} bound complex of **1** as presented in Scheme 3.

To optimize the conditions for practical applications in environmental and biological samples, the effect of water on the fluorescence emission of **1** in the absence and presence of Zn^{2+} were investigated in acetonitrile solutions. Figure 9 shows the effect of water content on the fluorescence behavior of **1** in acetonitrile solution. As the percentage of water is increased, an enhancement in the LE state emission intensity with the disappearance of PET promoted CT state is observed. At 20% water content, a single emission peak around 437 nm is observed. The disappearance of PET promoted CT state indicates the lesser extent of PET in these solvent mixtures. Addition of Zn^{2+} to the acetonitrile/water mixture solutions shows a fluorescence

dx.doi.org/10.1021/jp209061f |J. Phys. Chem. A 2011, 115, 14292–14299

enhancement without any spectral shift due to the suppression of PET process. The extent of enhancement was found to decrease with an increase in the water content (Figure 9). The optimum percentage of water for a better Zn^{2+} sensing was found to be 80:20 (acetonitrile/water, v/v) solvent mixture. Addition of Zn^{2+} to **1** in this solvent mixture shows a 4.5-fold fluorescence enhancement as shown in Figure 10. The observed lower extent of fluorescence enhancement compared to that in acetonitrile also further supports the decreased ease of PET in the acetonitrile/water mixtures. The detection limit was found to be 167 nM in acetonitrile:water (80:20, v/v) mixture, which is low when compared to the detection limit arrived in acetonitrile. The stability constant (Table 2) of **1**·Zn^{2+} complex was also found to be lower in acetonitrile/water (80:20, v/v), which reveals a weak binding interaction between BPA unit Zn^{2+} in these solvent mixtures.

IV. CONCLUSION

A new dual fluorescent ADD derivative (**1**) bearing BPA receptor has been synthesized and proved to be a highly selective and sensitive Zn^{2+} sensor. Binding of Zn^{2+} at the receptor moiety leads to the quenching of PET promoted CT state emission with an enhancement in the LE state intensity under a ratiometric manner. This ratiometric change is attributed to the suppression of PET process during the chelation of Zn^{2+} in a 1:1 complexation ratio. Fluorescence lifetime studies clearly prove the involvement PET process in the fluorescence signaling action. The observation of ratiometric fluorescence response under PET signaling mechanism will expand the scope on PET based sensors for the ratiometric detection. Sensing of Zn^{2+} is also achieved in a mixed acetonitrile/water solutions, which shows a single emission with an enhancement in the fluorescence intensity.

■ ASSOCIATED CONTENT

Supporting Information. NMR spectra, 3D-contour spectra of **1**; fluorescence lifetime decay of ADD dyes, emission spectra of **1** in the presence of various metal ions and Benesi–Hildebrand plot for **1** with Zn^{2+}. This material is available free of charge via the Internet at http://pubs.acs.org.

■ AUTHOR INFORMATION

Corresponding Author

*Tel.: 091-44-24540962. Fax: 091-44-24546709. E-mail: prm60@hotmail.com.

■ ACKNOWLEDGMENT

We thank the Department of Science and Technology (DST), Government of India, for financial support through SERC scheme Project No. DST/SR/S1/PC-31/2005. Financial support by DST-IRHPA is also gratefully acknowledged.

■ REFERENCES

(1) Auld, D. S. *BioMetals* **2001**, *14*, 271–313.

(2) (a) Bush, A. I. *Curr. Opin. Chem. Biol.* **2000**, *4*, 184–191. (b) Frederickson, C. J.; Koh, J.-Y.; Bush, A. I. *Nat. Rev. Neurosci.* **2005**, *6*, 449–462.

(3) Desvergne, J. P., Czarnik, A. W., Eds. *Chemosensors for Ion and Molecule Recognition*; Kluwer Academic Publishers: Dordrecht, The Netherlands, 1997.

(4) (a) Jiang, P.; Guo, Z. *Coord. Chem. Rev.* **2004**, *248*, 205–229. (b) Thompson, R. B. *Curr. Opin. Chem. Biol.* **2005**, *9*, 526–532. (c) Lim, N. C.; Freake, H. C.; Bruckner, C. *Chem.—Eur. J.* **2005**, *11*, 38–49. (d) Zhang, X.-A.; Lovejoy, K. S.; Jasanoff, A.; Lippard, S. J. *Proc. Natl. Acad. Sci. U.S.A.* **2007**, *104*, 10780–10785. (e) Nolan, E. M.; Lippard, S. J. *Acc. Chem. Res.* **2009**, *42*, 193–203. (f) Xu, Z.; Yoon, J.; Spring, D. R. *Chem. Soc. Rev.* **2010**, *39*, 1996–2006. (g) Li, W.; Nie, Z.; He, K.; Xu, X.; Li, Y.; Huang, Y.; Yao, S. *Chem. Commun.* **2011**, *47*, 4412–4414. (h) Liu, T.; Liu, S. *Anal. Chem.* **2011**, *83*, 2775–2785. (i) Huang, C.; Qu, J.; Qi, J.; Yan, M.; Xu, G. *Org. Lett.* **2011**, *13*, 1462–1465.

(5) (a) Burdette, S. C.; Walkup, G. K.; Spingler, B.; Tsien, R. Y.; Lippard, S. J. *J. Am. Chem. Soc.* **2001**, *123*, 7831–7841. (b) Gunnlaugsson, T.; Lee, T. C.; Parkesh, R. *Org. Biomol. Chem.* **2003**, *1*, 3265–3267. (c) Lu, X.; Zhu, W.; Xie, Y.; Li, X.; Gao, Y.; Li, F.; Tian, H. *Chem.—Eur. J.* **2010**, *16*, 8355–8364.

(6) (a) Xue, L.; Liu, C.; Jiang, H. *Chem. Commun.* **2009**, 1061–1063. (b) Hanaoka, K.; Muramatsu, Y.; Urano, Y.; Terai, T.; Nagano, T. *Chem.—Eur. J.* **2010**, *16*, 568–572.

(7) (a) Sclafani, J. A.; Maranto, M. T.; Sisk, T. M.; Van Arman, S. A. *Tetrahedron Lett.* **1996**, *37*, 2193–2196. (b) Kawakami, J.; Niiyama, T.; Ito, S. *Anal. Sci.* **2002**, *18*, 735–736.

(8) (a) Ambrosi, G.; Formica, M.; Fusi, V.; Giorgi, L.; Macedi, E.; Micheloni, M.; Paoli, P.; Pontellini, R.; Rossi, P. *Inorg. Chem.* **2010**, *49*, 9940–9948. (b) Majzoub, A. E.; Cadiou, C.; Dechamps-Olivier, I.; Tinant, B.; Chuburu, F. *Inorg. Chem.* **2011**, *50*, 4029–4038.

(9) (a) Wang, Z.; Palacios, M. A.; Zyryanov, G.; Anzenbacher, P., Jr. *Chem.—Eur. J.* **2008**, *14*, 8540–8546. (b) Han, Z.-X.; Zhang, X.-B.; Li, Z.; Gong, Y.-J.; Wu, X.-Y.; Jin, Z.; He, C.-M.; Jian, L.-X.; Zhang, J.; Shen, G.-L.; Yu, R.-Q. *Anal. Chem.* **2010**, *82*, 3108–3113.

(10) de Silva, A. P.; Gunaratne, H. Q. N.; Gunnlaugsson, T. A.; Huxley, T. M.; McCoy, C. P.; Rademacher, J. T.; Rice, T. E. *Chem. Rev.* **1997**, *97*, 1515–1566.

(11) (a) Walkup, G. K.; Burdette, S. C.; Lippard, S. J.; Tsien, R. Y. *J. Am. Chem. Soc.* **2000**, *122*, 5644–5645. (b) Buccella, D.; Horowitz, J. A.; Lippard, S. J. *J. Am. Chem. Soc.* **2011**, *133*, 4101–4114.

(12) (a) Burdette, S. C.; Frederickson, C. J.; Bu, W.; Lippard, S. J. *J. Am. Chem. Soc.* **2003**, *125*, 1778–1787. (b) Kiyose, K.; Kojima, H.; Urano, Y.; Nagano, T. *J. Am. Chem. Soc.* **2006**, *128*, 6548–6549. (c) Jiang, W.; Fu, Q.; Fan, H.; Wang, W. *Chem. Commun.* **2008**, 259–261. (d) You, Y.; Tomat, E.; Hwang, K.; Atanasijevic, T.; Nam, W.; Jasanoff, A. P.; Lippard, S. J. *Chem. Commun.* **2010**, *46*, 4139–4141.

(13) Kim, T. W.; Park, J.-H.; Hong, J.-I. *J. Chem. Soc., Perkin Trans. 2* **2002**, 923–927.

(14) (a) Zhang, L.; Clark, R. J.; Zhu, L. *Chem.—Eur. J.* **2008**, *14*, 2894–2903. (b) Schwarze, T.; Muller, H.; Dosche, C.; Klamroth, T.; Mickler, W.; Kelling, A.; Lohmannsroben, H.-G.; Saalfrank, P.; Holdt, H.-J. *Angew. Chem., Int. Ed.* **2007**, *46*, 1671–1674. (c) Xu, Z.; Kim, G.-H.; Han, S. J.; Jou, M. J.; Lee, C.; Shin, I.; Yoon, J. *Tetrahedron* **2009**, *65*, 2307–2312. (d) Schwarze, T.; Mickler, W.; Dosche, C.; Flehr, R.; Klamroth, T.; Lohmannsroben, H.-G.; Saalfrank, P.; Holdt, H.-J. *Chem.—Eur. J.* **2010**, *16*, 1819–1825. (e) Bozdemir, O. A.; Guliyev, R.; Buyukcakir, O.; Selcuk, S.; Kolemen, S.; Gulseren, G.; Nalbantoglu, T.; Boyaci, H.; Akkaya, E. U. *J. Am. Chem. Soc.* **2010**, *132*, 8029–8036.

(15) Lakowicz, J. R. *Probe Design and Chemical Sensing, Topics in Fluorescence Spectroscopy*; Plenum: New York, 1994; Vol. 4.

(16) (a) Zhou, Z. G.; Yu, M. X.; Yang, H.; Huang, K. W.; Li, F. Y.; Yi, T.; Huang, C. H. *Chem. Commun.* **2008**, 3387–3389. (b) Roussakis, E.; Pergantis, S. A.; Katerinopoulos, H. E. *Chem. Commun.* **2008**, 6221–6223. (c) Wang, H.-H.; Xue, L.; Qian, Y.-Y.; Jiang, H. *Org. Lett.* **2010**, *12*, 292–295. (d) Xu, Z.; Yoon, J.; Spring, D. R. *Chem. Commun.* **2010**, *46*, 2563–2565. (e) Liu, Z.; Zhang, C.; He, W.; Yang, Z.; Gao, X.; Guo, Z. *Chem. Commun.* **2010**, *46*, 6138–6140. (f) Yu, H.; Xiao, Y.; Guo, H.; Qian, X. *Chem.—Eur. J.* **2011**, *17*, 3179–3191.

(17) (a) Woodroofe, C. C.; Lippard, S. J. *J. Am. Chem. Soc.* **2003**, *125*, 11458–11459. (b) Ajayaghosh, A.; Carol, P.; Sreejith, S. *J. Am. Chem. Soc.* **2005**, *127*, 14962–14963. (c) Lim, N. C.; Schuster, J. V.; Porto, M. C.; Tanudra, M. A.; Yao, L.; Freake, H. C.; Bruckner, C. *Inorg. Chem.* **2005**, *44*, 2018–2030. (d) Xu, Z.; Qian, X.; Cui, J.; Zhang, R.

Tetrahedron **2006**, *62*, 10117–10122. (e) Zhang, Y.; Guo, X.; Si, W.; Jia, L.; Qian, X. *Org. Lett.* **2008**, *10*, 473–476. (f) Liu, Z.; Zhang, C.; Li, Y.; Wu, Z.; Qian, F.; Yang, X.; He, W.; Gao, X.; Guo, Z. *Org. Lett.* **2009**, *11*, 795–798. (g) Xue, L.; Liu, Q.; Jiang, H. *Org. Lett.* **2009**, *11*, 3454–3457. (h) Ito, H.; Matsuoka, M.; Ueda, Y.; Takuma, M.; Kudo, Y.; Iguchi, K. *Tetrahedron* **2009**, *65*, 4235–4238. (i) Taki, M.; Watanabe, Y.; Yamamoto, Y. *Tetrahedron Lett.* **2009**, *50*, 1345–1347. (j) Xue, L.; Liu, C.; Jiang, H. *Chem. Commun.* **2009**, 1061–1063. (k) Zhou, X.; Lu, Y.; Zhu, J.-F.; Chan, W.-H.; Lee, A. W. M.; Chan, P.-S.; Wong, R. N. S.; Mak, N. K. *Tetrahedron* **2011**, *67*, 3412–3419.

(18) (a) Thiagarajan, V.; Ramamurthy, P.; Thirumalai, D.; Ramakrishnan, V. T. *Org. Lett.* **2005**, *7*, 657–660. (b) Ashokkumar, P.; Ramakrishnan, V. T.; Ramamurthy, P. *Eur. J. Org. Chem.* **2009**, 5941–5947. (c) Koteeswari, R.; Ashokkumar, P.; Ramakrishnan, V. T.; Padma Malar, E. J.; Ramamurthy, P. *Chem. Commun.* **2010**, *46*, 3268–3270. (d) Ashokkumar, P.; Ramakrishnan, V. T.; Ramamurthy, P. *J. Phys. Chem. B* **2011**, *115*, 84–92. (e) Koteeswari, R.; Ashokkumar, P.; Padma Malar, E. J.; Ramakrishnan, V. T.; Ramamurthy, P. *Chem. Commun.* **2011**, *47*, 7695–7697.

(19) Kumaran, R.; Ramamurthy, P. *J. Phys. Chem. B* **2006**, *110*, 23783–23789.

(20) (a) Job, P. *Ann. Chem.* **1928**, *9*, 113–203. (b) Gil, V. M. S.; Oliveira, N. C. *J. Chem. Educ.* **1990**, *67*, 473–478. (c) Loukas, Y. L. *Analyst* **1997**, *122*, 377–381.

(21) (a) Shanmugasundaram, P.; Murugan, P.; Ramakrishnan, V. T.; Srividya, N.; Ramamurthy, P. *Heteroat. Chem.* **1996**, *7*, 17–22. (b) Srividya, N.; Ramamurthy, P.; Shanmugasundaram, P.; Ramakrishnan, V. T. *J. Org. Chem.* **1996**, *61*, 5083–5089.

(22) (a) Thiagarajan, V.; Selvaraju, C.; Padmamalar, E. J.; Ramamurthy, P. *ChemPhysChem* **2004**, *5*, 1200–1209. (b) Ashokkumar, P.; Thiagarajan, V.; Vasanthi, S.; Ramamurthy, P. *J. Photochem. Photobiol., A* **2009**, *208*, 117–124.

(23) (a) Long, G. L.; Winefordner, J. D. *Anal. Chem.* **1983**, *55*, 712A–724A. (b) Pandey, S.; Azam, A.; Pandey, S.; Chawla, H. M. *Org. Biomol. Chem.* **2009**, *7*, 269–279.

(24) Fernandez-Gutierrez, A.; Munoz de la Pena, A. In *Molecular Luminescence Spectroscopy. Methods and Applications*; Schulman, S. G., Ed.; Wiley: New York, 1985; Part 1, p 371; (b) Bourson, J.; Pouget, J.; Valeur, B. *J. Phys. Chem.* **1993**, *97*, 4552–4557.

(25) Benesi, H. A.; Hildebrand, J. H. *J. Am. Chem. Soc.* **1949**, *71*, 2703–2707.

(26) (a) Royzen, M.; Durandin, A.; Young, V. G., Jr.; Geacintov, N. E.; Canary, J. W. *J. Am. Chem. Soc.* **2006**, *128*, 3854–3855. (b) Michaels, H. A.; Murphy, C. S.; Clark, R. J.; Davidson, M. W.; Zhu, L. *Inorg. Chem.* **2010**, *49*, 4278–4287.

(27) (a) Srividya, N.; Ramamurthy, P.; Ramakrishnan, V. T. *Spectrochim. Acta A* **1997**, *53*, 1743–1753. (b) Srividya, N.; Ramamurthy, P.; Ramakrishnan, V. T. *Spectrochim. Acta A* **1998**, *54*, 245–253.